Research Square

Preprints are preliminary reports that have not undergone peer review.
They should not be considered conclusive, used to inform clinical practice,
or referenced by the media as validated information.

Controls of Multi-stage Tectonic Evolution on Gold Mineralization in Western Guangdong, South China

Wei Quan
Changsha General Survey of Natural Resources Centre, China Geological Survey
Tao Xiao
Changsha General Survey of Natural Resources Centre, China Geological Survey
Yuxuan Huang
School of Geosciences and Info-Physics, Central South University
Mohammed Ibrahim
School of Geosciences and Info-Physics, Central South University
Zhihao Sun
School of Geosciences and Info-Physics, Central South University
Buqing Wang
Changsha General Survey of Natural Resources Centre, China Geological Survey
Huan Li
lihuan@csu.edu.cn

School of Geosciences and Info-Physics, Central South University

Article

Keywords: metallogenic structures, Qin-Hang metallogenic belt, tectonic evolution, western Guangdong, deep ore prospecting, gold deposits

Posted Date: October 21st, 2025

DOI: https://doi.org/10.21203/rs.3.rs-7612237/v1

License: This work is licensed under a Creative Commons Attribution 4.0 International License.
Read Full License

Additional Declarations: No competing interests reported.

Article

Controls of Multi-stage Tectonic Evolution on Gold Mineralization in Western Guangdong, South China

Wei Quan [1], Tao Xiao [1]*, Yuxuan Huang [2], Mohammed Abdalla Elsharif Ibrahim [2], Zhihao Sun [2], Buqing Wang [1] and Huan Li [2]*

[1] Changsha General Survey of Natural Resources Centre, China Geological Survey, Changsha 410600, China; quanwei@mail.cgs.gov.cn (W.Q.); xiaotao@mail.cgs.gov.cn (T.X.); wwbq555@zuaa.zju.edu.cn (B.W.)
[2] School of Geosciences and Info-Physics, Central South University, Changsha 410083, China; 255006003@csu.edu.cn (Y.H.); 215008015@csu.edu.cn (M.A.E.I); 245011071@csu.edu.cn (Z.S); lihuan@csu.edu.cn (H.L.);
* Correspondence: xiaotao@mail.cgs.gov.cn (T. Xiao); lihuan@csu.edu.cn (H. Li)

Abstract: Western Guangdong, situated in the southern segment of the Qin-Hang metallogenic belt (South China), hosts significant gold deposits associated with deep fault intersections and intense magmatic, metamorphic and tectonic activities, making it highly prospective for mineral exploration. Previous studies focused on metallogenic geochemistry and granite structures, but systematic research on structural controls and tectonic evolution governing gold emplacement remains limited. This work analyzes Paleozoic-Mesozoic outcrops through structural mapping, geometric-kinematic analysis of deformation styles, and orientation statistics to reconstruct polyphase tectonic evolution. Four major events are identified: (a) Early Paleozoic NW-SE compression (dip directions of 258°-350° & 90°-190°), (b) Triassic NE-SW compression (dip directions of 133°-266° & 4°-66°), (c) Jurassic NW-SE compression (dip directions of 123°-174° & 295°-325°), and (d) Cretaceous NW-SE extension (dip directions of 90°-160° & 280°-331°). The four major tectonic events provide a robust framework for predicting favorable gold exploration targets in the region, and underscores the critical importance of understanding regional tectonic evolution in metallogenic studies.

Keywords: metallogenic structures; Qin-Hang metallogenic belt; tectonic evolution; western Guangdong; deep ore prospecting; gold deposits.

1. Introduction

The western Guangdong region, located in the southern section of the Qin-Hang metallogenic belt (Fig. 1), represents a key gold mineralization zone in South China, with significant prospecting potential. Since the 1990s, numerous studies have examined various aspects of gold mineralization in this region, including the timing of granitic activities and mineralization, geological characteristics of mineralization, ore-forming fluid properties, metal sources, mineralization processes, and ore genesis [1-4]. However, the research in the western Guangdong region remains relatively underdeveloped, and a deeper understanding of the mineralization conditions, controlling factors, and the roles of ductile versus brittle deformation is still needed. In particular, the relationship between the mylonite belt, metamorphic rock series, and their associated structures with gold mineralization has yet to be clearly and systematically understood. Prospecting efforts have predominantly concentrated on areas surrounding previously identified mines, with insufficient

depth achieved in exploration. Moreover, systematic research on the regional structural controls of mineralization and orebody patterns has not been conducted. As a result, the limited existing studies have not succeeded in developing or establishing applicable prospecting models for this region. This study aims to: (1) systematically analyze the strata structural architecture of the western Guangdong region; (2) establish the sequence of deformation events and associated stress fields; (3) determine the relationship between structural evolution and gold mineralization; and (4) provide a structural framework for guiding future exploration in the region.

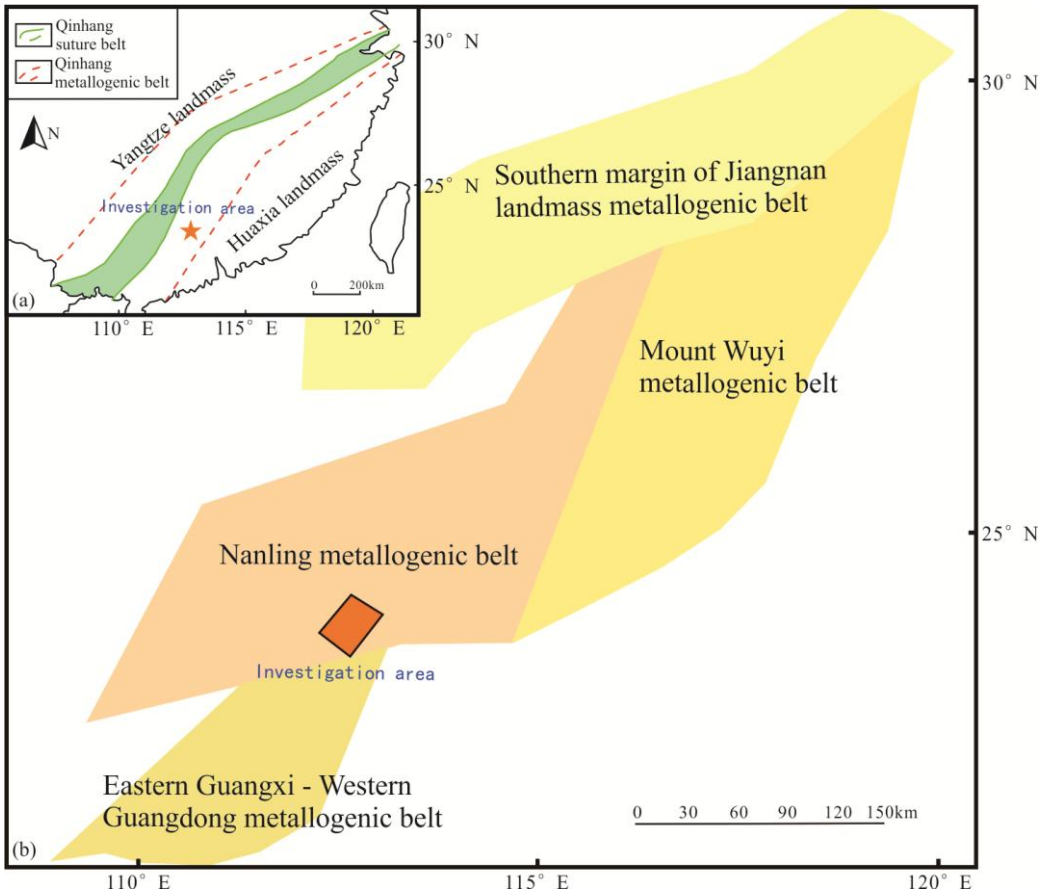


Figure 1. Map showing the major metallogenic belts in South China and the location of the study area (i.e., western Guangdong region).

2. Geological Features of the Western Guangdong Region

The South China Block was formed by collision between the Yangtze Block and Cathaysia Block in the Neoproterozoic and subsequently experienced four important Phanerozoic tectonic events: the Wuyi-Yunkai Movement (Early Paleozoic), the Emeishan flood basalt magmatism (Late Paleozoic), the Indosinian Movement (Triassic), and the Yanshanian Movement (Jurassic-Cretaceous).

The gold mining area in western Guangdong is part of the Huaiji Block within the Huaxia landmass' geological framework, situated at the boundary between the northeastern part of the Yunkai uplift and the western margin of the central Guangdong depression (Fig. 2). The area is characterized by a complex sedimentary history and intense magmatic, metamorphic, and tectonic activities [5,6]. These favorable geological conditions for mineralization make it a significant and highly prospective metallogenic belt for precious metals in South China. More specifically, the western Guangdong region has undergone multiple tectonic events, including those in the Early Paleozoic, Triassic, and Jurassic-Cretaceous.

Faults in the study area are primarily normal and reverse in type, with dominant strikes in the northeast, north-northeast, and nearly north-south directions, while east-west orientations are relatively rare. Notably, northeast-trending faults have evolved into major deep-seated fault zones, such as the Guangning- Luoding fault (Fig. 2).

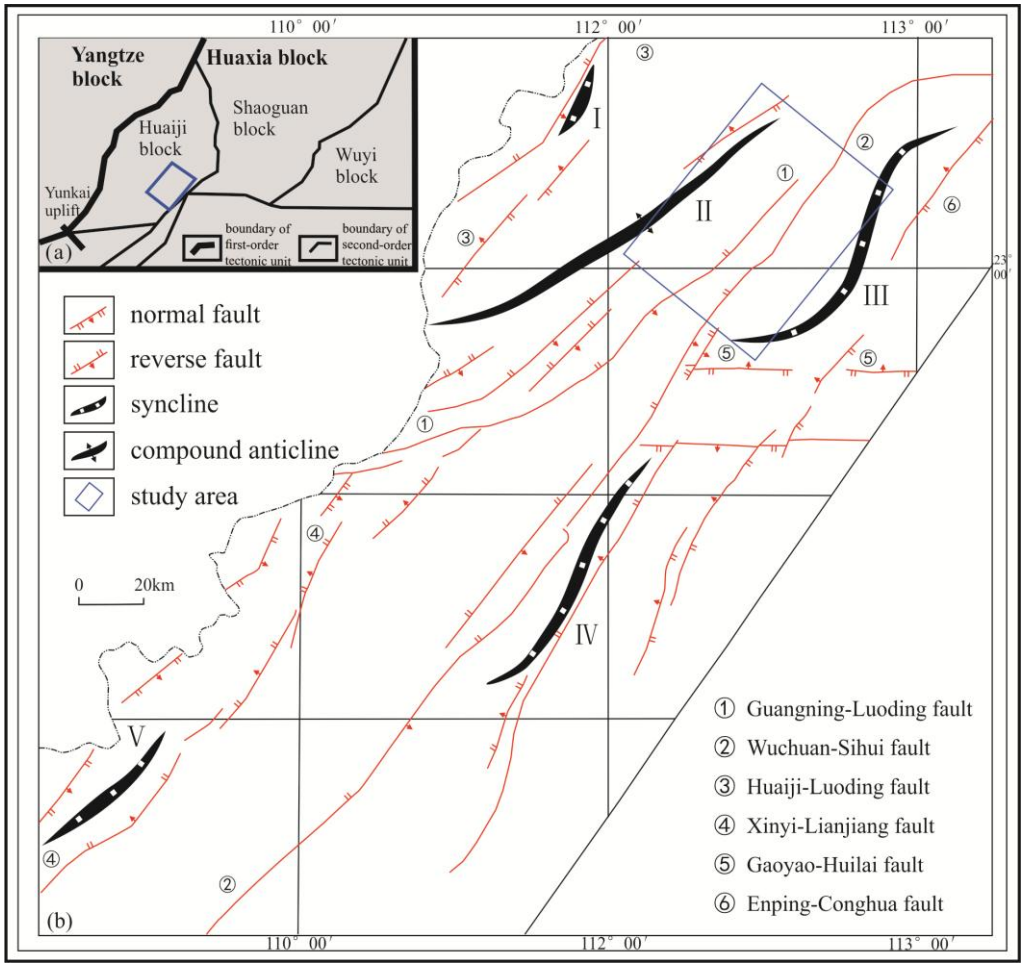


Figure 2. (a) Regional map showing the major tectonic units; (b) Detailed map illustrating the main structural elements in the western Guangdong region.

The area features well-exposed stratigraphic sequences ranging from the Neoproterozoic to the Cenozoic. The Neoproterozoic and Early Paleozoic strata consist of shallow to semi-deep marine flysch type clastic sediments. Influenced by Early Paleozoic tectonic movements, these rocks underwent regional low-grade metamorphism and significant deformation, while still preserving sedimentary characteristics, such as original stratification and sedimentary fabric. The Upper Paleozoic strata comprised limited platform to open platform facies and delta-front to coastal carbonate rock sediments. The Upper Triassic to Lower Jurassic sequences are marked by interactions between lacustrine and terrestrial environments, resulting in lacustrine clastic rocks deposition. In contrast, the Lower Cretaceous is characterized by foothill river facies (Fig. 3). The main lithologies in the region include gray-green, gray-black medium-thick layered medium-fine grained feldspar quartz sandstone, lithic quartz sandstone, feldspar quartz greywacke, intercalated with sandy siltstone, siltstone, sericite phyllite, and carbonaceous phyllite.

The region also develops significant magmatic activity, predominantly during the Early Paleozoic and Jurassic-Cretaceous periods [7,8]. This magmatism is mainly intrusive in nature, dominanted by granitic rocks, with limited occurrences of volcanic rocks. The intrusive bodies primarily formed during the Ordovician, Permian, Triassic, and Jurassic

periods, with the Jurassic period being the most dominant. The main rock type is biotite adamellite, followed by hornblende biotite adamellite and minor biotite syenogranite. Additionally, small volumes of quartz porphyry, granite pegmatite, fine-grained rocks, diorite porphyry, and porphyrite are present, typically occurring as small plutons, veins, or dikes.

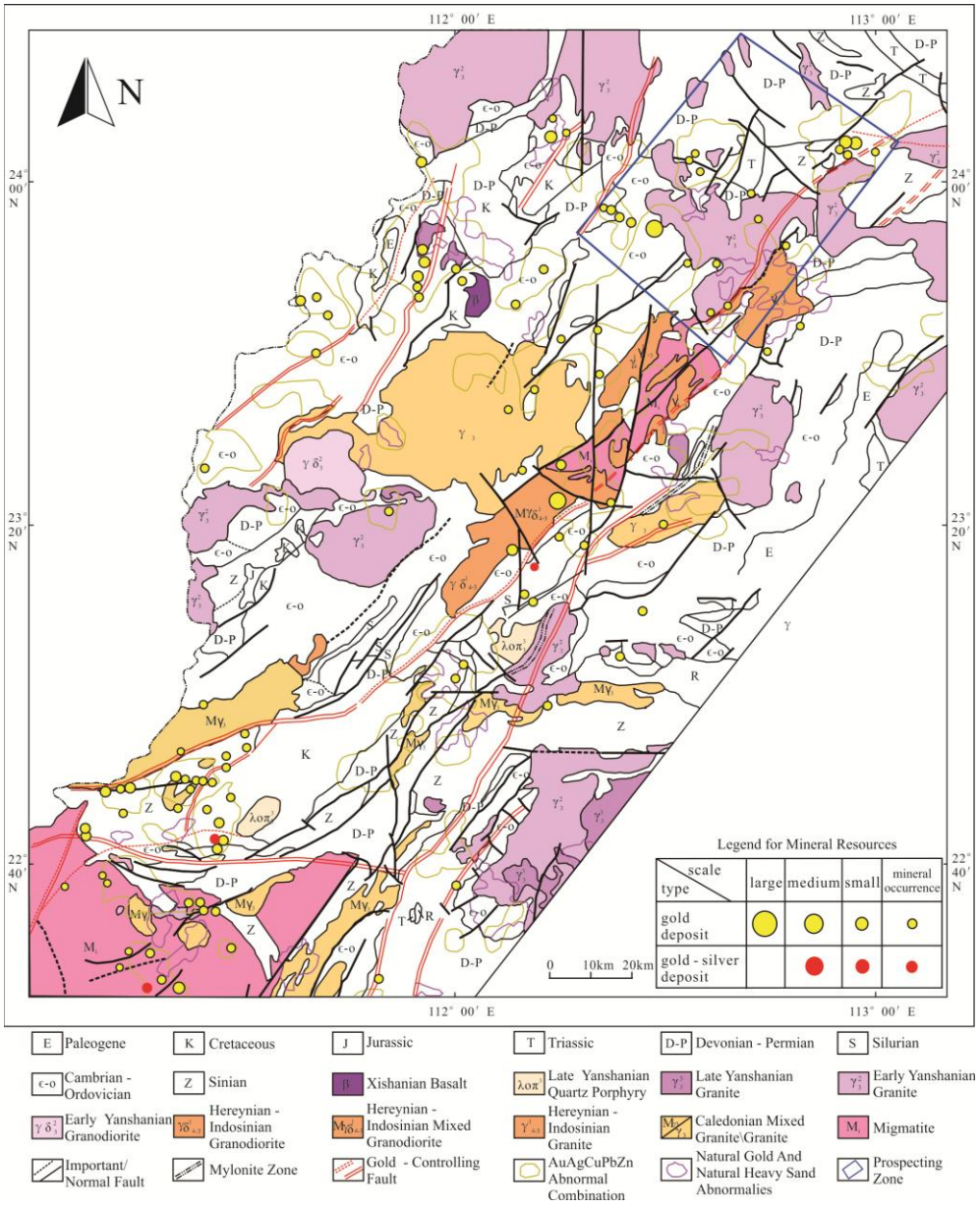


Figure 3. Regional geological and mineral resources map of western Guangdong gold mining area.

Mineralization in the western Guangdong region is widespread. Previous studies suggest that the Precambrian continental crust served as the primary source of mineral-forming components for the hydrothermal systems responsible for the gold deposits [9,10]. The Yunkai area and its northwestern margin host gold, silver, copper, lead, zinc, and other metals, primarily associated with metamorphic rock formations of Sinian and Early Cambrian ages [11,12]. Studies have shown that the Early Paleozoic Epoch was a key metallogenic period for gold deposits in the region [13]. Additionally, copper, lead, and zinc deposits are found in shallow marine carbonate rocks of the Upper Paleozoic period. High-temperature hydrothermal mineralization is obvious [14], and magmatic

activity is closely related to the formation of ore minerals (such as iron, copper, lead, and zinc) and precious metals (like gold and silver) [8]. Most mineral deposits are located in the granite contact zones and are primarily associated with Jurassic- Cretaceous magmatism. Multi-phase magmatic events, particularly those during the Cretaceous Epoch, are closely linked to gold mineralization [15]. Quartz veins are widespread throughout the strata; however, their abundance varies significantly across the region [16].

3. Research Methods and Data Processing Procedures

This study primarily employed field mapping and structural analysis. Field measurements and recordings of the structural features were conducted for Paleozoic-Mesozoic strata in the region, and the data were processed using Orient software for statistical analysis and mapping. Systematic identification and geometric and kinematic analyses were then performed, using the mapped structural occurrences across different geological periods. These analyses allow us to unravel the superposition of different tectonic stages. Finally, the structural stress fields for each stage were restored using classical inversion methods.

4. Structural Analysis and Tectonic Deformation Stages

Based on geological background and previous studies on the tectonic evolution recorded by granites in the western Guangdong region [17], we have conducted field mapping and structural analysis for the Paleozoic-Mesozoic strata. Structural analysis reveals that the western Guangdong region has undergone four major tectonic events: 1. Early Paleozoic NW-SE compression; 2. Triassic NE-SW compression; 3. Jurassic NW-SE compression; and 4. Cretaceous NW-SE extension (see supplementary figure 1).

4.1. Early Paleozoic NW-SE compression

The results indicate that the earliest NW-SE compression in the study area occurred during the Early Paleozoic Epoch and was characterized by intense tectonic activity. This deformation episode was dominated by extensive development of folds, with NE-SW trending fault systems being the primary structural elements and folding playing a subordinate role. The NE-trending faults constitute the main structural framework of the study area, which includes ductile and brittle faults. They have different degrees of control or destruction over regional geological processes, including sedimentation, magmatism, metamorphism, and mineralization in the region. Cataclastic rocks and structural lenses are developed along the NE-trending brittle fault zones, accompanied by localized silicification that suggests syn-deformational fluid circulation. The NE-trending brittle faults are generally reverse faults, consistent with the compressional stress regime. Although ductile faults in this area exhibit a primary NE-trending, they are strongly distorted, with their orientations and dip directions modified by subsequent episodes of ductile shear deformation. At a macroscopic scale, the NW-SE compression led to the formation of a large NE-SW trending anticline (Fig. 2, anticline II), which forms a significant component of the regional structural framework.

Field observations reveal that derived structures from the NE-SW trending large anticlines include a series of compressional cleavages, shear joints, and early nearly NE-trending quartz veins that filled tensile spaces between foliation planes or shear planes. Compressional cleavages are well developed along both flanks of the NE-SW trending folds, indicating intense horizontal compressional tectonic forces (Fig. 4). The systematic variation in cleavage orientation across the anticline provides robust evidence for the stress field orientation: dip directions of early compressional cleavages in the western and northwestern limbs of the anticline range from 270 ° -350 °, with dip angles between 40 °

-80 °. In contrast, the dip directions in the southeastern limb range from 90 ° -190 °. This geometric arrangement demonstrates that the western Guangdong region experienced significant NW-SE compression during the Early Paleozoic Epoch.

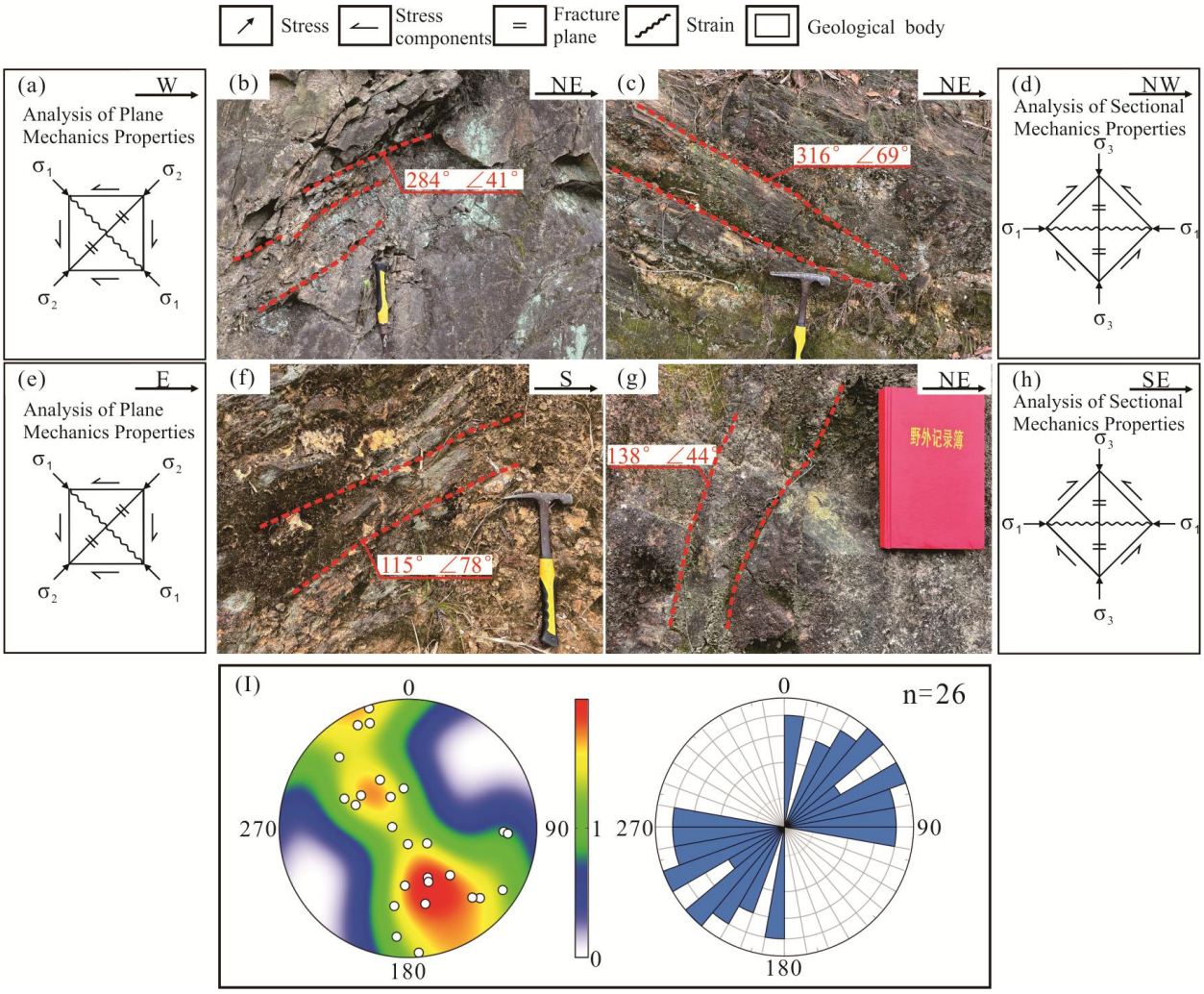


Figure 4. (a) Analysis of the plane and sectional mechanics properties of the compressional cleavages of the northwest limb of the anticline; (b and c) Penetrative compressional cleavages in Cambrian strata on the northwest flank of the anticline; (d) Analysis of the plane and sectional mechanics properties of the compressional cleavages of the northwest limb of the anticline; (f and g) Strong compressional cleavages in Cambrian strata on the southeastern flank of the anticline; (e and h) Analysis of plane and sectional mechanics properties of the compressional cleavages of the southeast wing of the anticline; (i) Projection map and rose diagram illustrating the dip directions and trends of NW-SE trending compressional cleavages during the Early Paleozoic period.

Using the measured data from the study area, the classical inversion method and the foliation rose diagram analysis (Fig. 4) were applied to reconstruct the paleotectonic stress field of this period. The results indicate that during the Early Paleozoic NW-SE compression deformation stage, the maximum principal stress (σ1) was oriented approximately NW-SE; while the minimum principal stress (σ3) was oriented NE-SW. This stress configuration is consistent with regional tectonic models for the South China Block during the Early Paleozoic.

Multiple generations of quartz veins provide additional constraints on the deformation history. In the Cambrian metamorphic sandstone layers with compressional cleavages dipping NW and SE, quartz veins are observed along bedding planes and foliations.

These quartz veins occur in multiple sets, are often thin and occasionally form clusters (Fig. 5a, b, c). Their trending directions range from 200 ° -340 °, further indicating the influence of Early Paleozoic NW-SE compression since their development along NE-SW-trending cleavage formed by NW-SE compression during the Early Paleozoic. Significantly, these veins show no evidence of overprinting by later tectonic events with different stress orientations (Fig. 6b, c), suggesting they represent primary structures related to the Early Paleozoic compression.

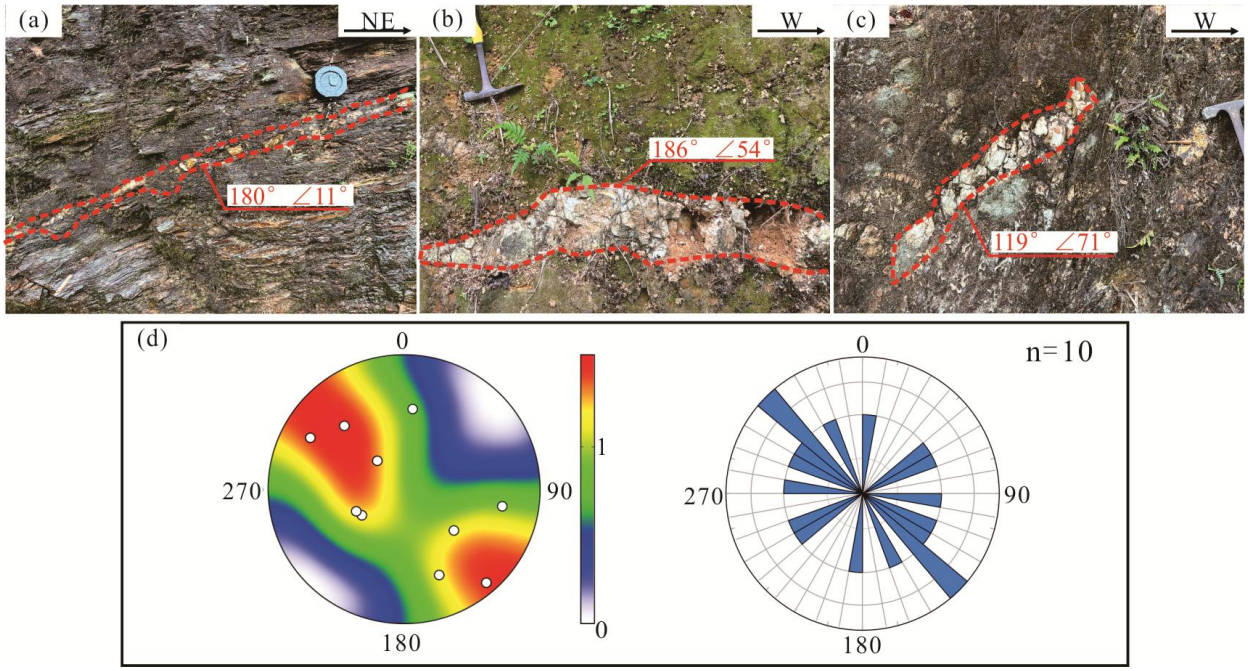


Figure 5. (a, b, and c) Quartz veins in the Cambrian strata on the southeastern flank of the anticline; (d) Projection map and rose diagram showing the occurrence of Early Paleozoic quartz veins in the research area (dip direction).

Joint analysis supports the interpreted stress field, with multiple sets observed in the field outcrops. In the southwest wing, joints display dip directions ranging from 193° to 266 ° and dip angles between 28° and 70°. In the northeast wing, joints exhibit dip directions from 36° to 66° and dip angles between 86° and 88° (Fig. 6). These joint orientations are consistent with formation under NW - SE compression during the Early Paleozoic Epoch (Fig. 6g).

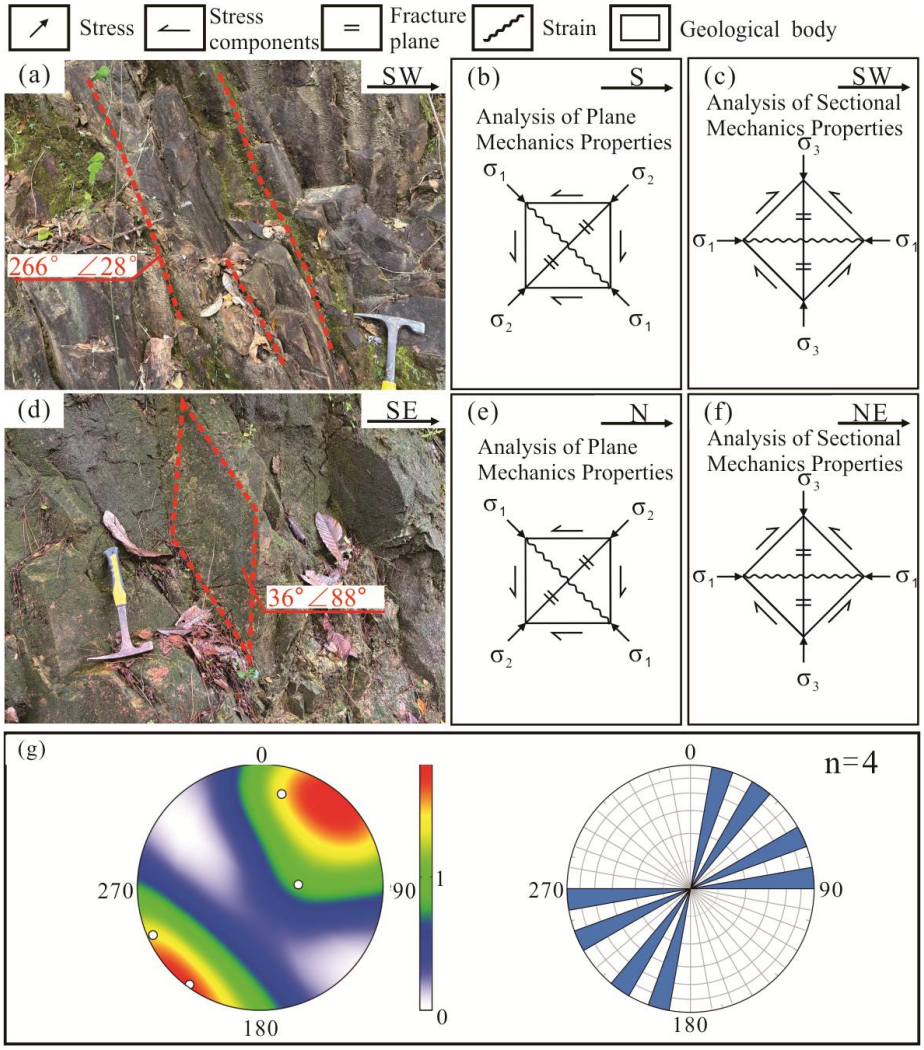


Figure 6. (a) Joints observed on the southwest flank of the anticline; (b and c) Analysis of plane and sectional mechanical properties of joints on the southwest flank of the anticline; (d) Joints observed on the northeast flank of the anticline; (e and f) Analysis of plane and sectional mechanical properties of joints on the northeast flank of the anticline; (g) Projection Map and rose diagram depicting joint occurrences during the Early Paleozoic Epoch in the research area (dip direction).

4.2. Triassic NE-SW compression

The Triassic period witnessed a fundamental change in the regional stress field, with the development of NE-SW compression that resulted in the formation of a large NW-SE trending anticline in the study area. The two limbs of this anticline are mainly composed of the Cambrian Niujiaohe Formation and the Cambrian Gaotan Formation. This structure is superimposed on the earlier northeast-trending anticline formed during the Early Paleozoic, forming a complex dome structure (see supplementary Figure 1a). The derived structures of large NW-SE trending anticlines observed in field outcrops mainly include compressional cleavages, shear joints, and nearly NW-trending quartz veins that fill tensile spaces between foliation and shear planes.

The NW-SE trending anticline shows well-developed compressional cleavages on both limbs, indicating strong NE-SW compressional forces in the horizontal direction. In the Cambrian strata on the western and southwestern limbs of the anticline, the dip directions of these structures range from 133° to 261°, while on the southeastern limb, the dip directions of compressional cleavages vary from 4° to 47° (Fig. 7).

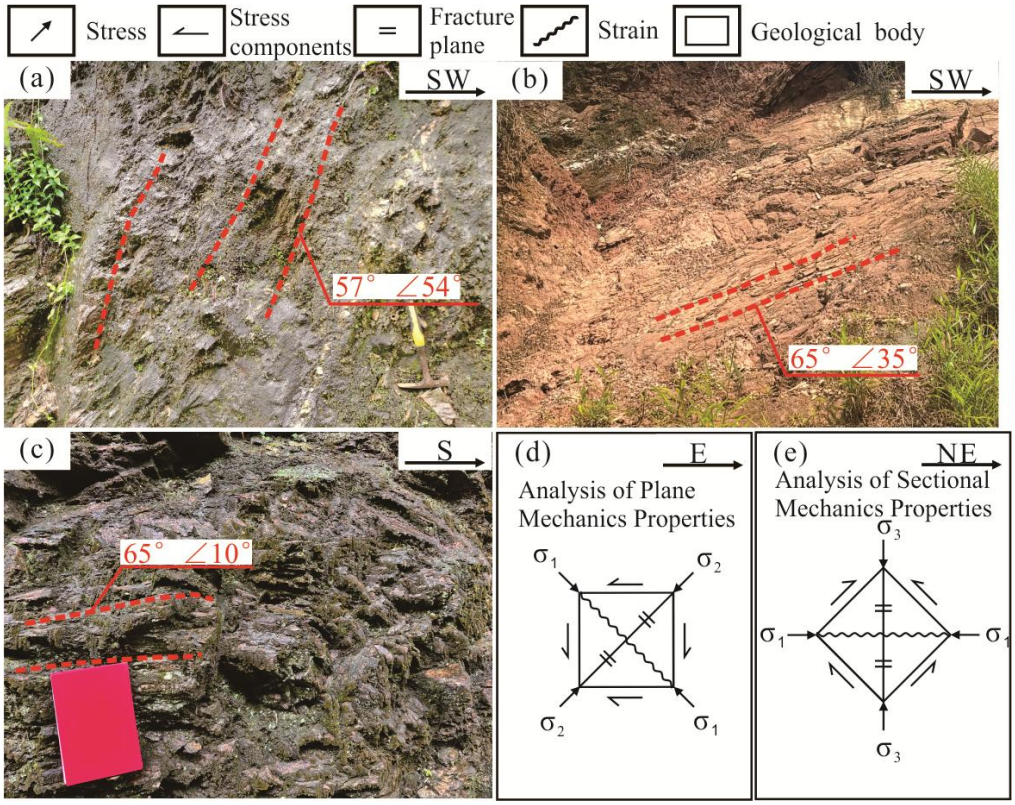


Figure 7. (a and b) Compressional cleavages in the Cambrian strata on the northeast flank of the anticline; (c) The cleavages in the Cambrian strata on the northeast flank of the anticline; (d and e) Analysis of plane and sectional mechanical properties of compressional cleavages in the Cambrian strata on the northeast flank of the anticline.

Localized structural displacement is marked by NE- and SW-dipping compressional cleavages intersecting or transforming the NW and SE-dipping compressional cleavages from the early Paleozoic, resulting in fracturing or the development of traction structures (Fig. 8a). In the Cambrian Niujiaohe Formation on the western flank of the anticline, three distinct cleavage sets with varying orientations are observed, each reflecting separate tectonic events. A set of NW-dipping cleavages was displaced by a subsequent set of NE-dipping cleavages, which was in turn displaced by another NW-dipping set (Fig. 8b). The earliest NW-dipping cleavage resulted from NW-SE compression during the Early Paleozoic. This suggests that the NE-dipping cleavage in the region formed after the Early Paleozoic but before the Jurassic NW-SE compression that created the subsequent NW-dipping set. These observations indicate that the western Guangdong region underwent significant NE-SW compression during the Triassic period.

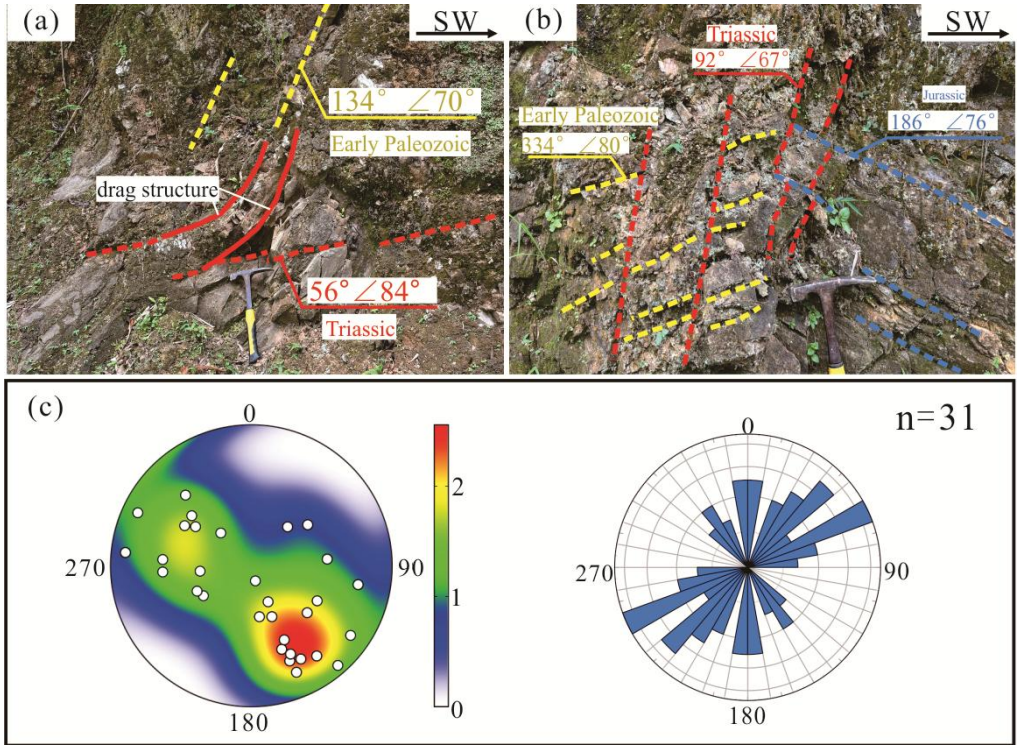


Figure 8. (a)Triassic and Early Paleozoic tectonic superposition outcrops; (b) Jurassic, Triassic, and Early Paleozoic tectonic superposition outcrops; (c) Map showing the distribution of Triassic cleavage in the research area (trend) and rose diagram illustrating the dip direction of Triassic cleavage in the research area.

Based on the measured data from the study area, the classical inversion method and the foliation rose diagram analysis (Fig. 8c) were utilized to invert the paleotectonic stress field of this period. The inversion results reveal that, during the Triassic NE-SW compression deformation stage, the maximum principal stress direction σ1 was approximately NE-SW; while the minimum principal stress direction σ3 approximately NW-SE (Fig. 8c). This represents approximately 90° rotation from the Early Paleozoic stress field, indicating a fundamental change in the regional tectonic regime.

In the Cambrian strata on the southeast wing of the NE-SW trending anticline, quartz veins are observed along the foliations or in deformed positions, displaying shear that obliquely crosses the foliation and extends upward from the hanging wall (Fig. 9a). These relationships indicate that these quartz veins formed after the NW-SE compression of the Early Paleozoic but prior to the NE-SW compression of the Triassic, classifying them as early NE-trending quartz veins.

Multiple quartz veins are present on both wings of the large NW-SE trending anticline, exhibiting different characteristics that reflect their formation timing. Some of these veins fill tensile spaces between two shear planes, forming lens-shaped structures. The quartz veins that developed along foliations are thin and formed after the NE-SW compression during the Triassic, displaying an NW orientation (Fig. 9b, c). In contrast, veins that fill tensile spaces between shear planes are wide and often appear in clusters, with some containing white mica. These shear planes correspond to the NW-SE compression of the Early Paleozoic and the NE-SW compression movement of the Triassic, respectively.

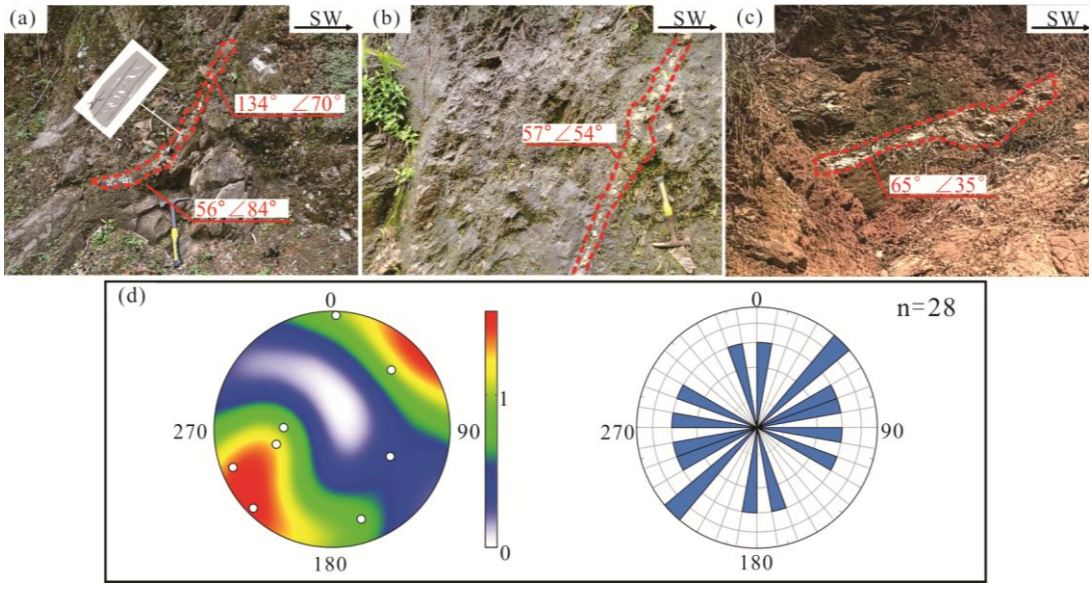


Figure 9. (a) cleavages in the Cambrian Niujiaohe Formation developed during two distinct stages, with slightly wider lens-shaped quartz veins filling the tensional space between two shear planes; (b) Quartz veins developed in the Cambrian Niujiaohe Formation strata; (c) Mica-bearing quartz veins developed in the Cambrian Gaotan Formation strata; (d) Map showing the dip direction of Triassic quartz veins in the research area and rose diagram illustrating the dip direction of Triassic quartz veins in the research area.

Multiple sets of joints are well developed in Cambrian rock layers exposed in the field. On the northwest wing, the joints have dip directions ranging from 258 ° to 315 °, with dip angles between 52 °-83 ° (Fig. 10). On the southeast wing, the dip directions mainly range from 145 °-173 °, with dip angles from 16 °-89 °, indicating the influence of Triassic NW-SE compression (Fig. 10b and c).

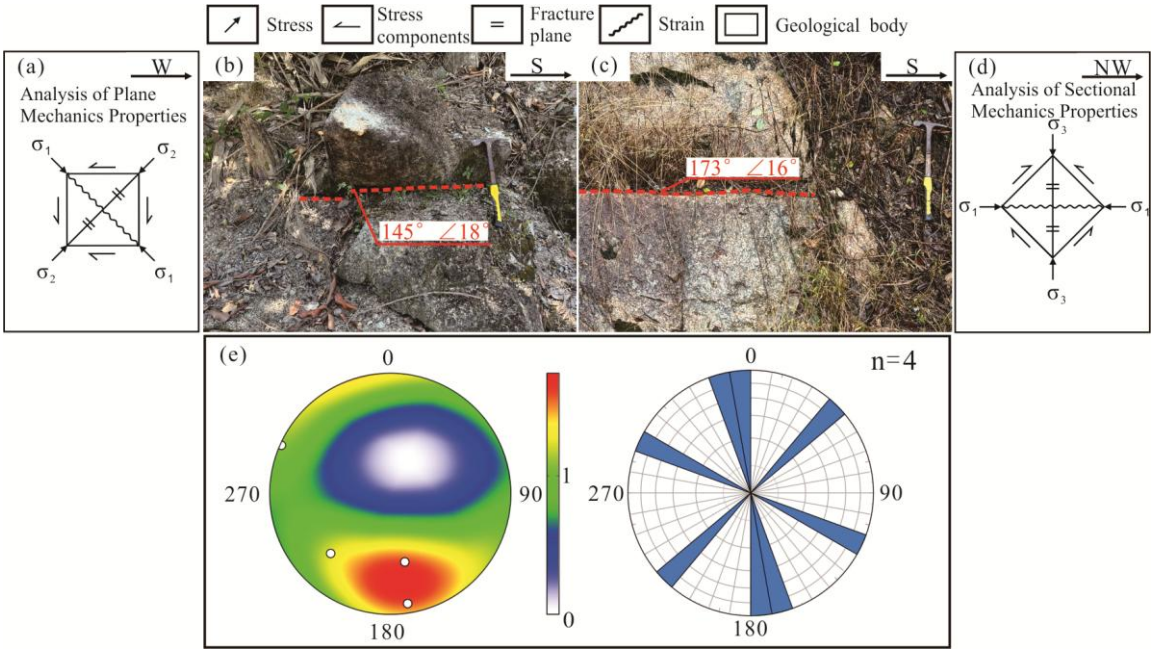


Figure 10. (b)(c)Joints in the Cambrian strata on the southeastern flank of the anticline ‖ (see Fig 2); (a)(d) Analysis of plane and sectional mechanics properties of joints in the Cambrian strata on the southeastern flank of the anticline; (e) Rose diagram and projection map showing the occurrence of joint during the Triassic Epoch in the research area (dip direction).

4.3. Jurassic NW-SE compression

The Jurassic NW-SE compression enhanced the NE-SW structural trend in western Guangdong (see supplementary figure), transforming the NE-SW structures from the Early Paleozoic and the NW-SE structures from the Triassic. This deformation episode represents the third major compressional event in the regional tectonic history and demonstrates the cyclical nature of stress field orientations in this part of the South China Block. Structural features indicative of Early Jurassic-Cretaceous movements, as observed in the field outcrops, primarily include compressional cleavages and quartz veins that either fill or modify early foliation planes or occur between compressional foliation planes.

The compressional cleavages formed during Jurassic deformation in the southeastern flank of the anticline show dip directions between 123° and 174° and dip angles ranging from 50° to 84°. On the northwest wing of the anticline, compressional cleavages show dip directions between 295° and 325°, with dip angles from 49° to 84°, systematically intersecting or modifying the cleavages formed by Early Paleozoic or Triassic movements. Furthermore, critical field relationships are observed in the Cambrian strata, where two sets of cleavages representing different deformation stages can be identified: early cleavages with NE or SW dip directions are intersected by later cleavages with SE dip directions (Fig. 11a). The early NE- or SW-dipping cleavages were produced by NW-SE compression during the Triassic, while their intersection by subsequent NW-SE compression movement, attributed to the Jurassic period, later affected the western Guangdong region.

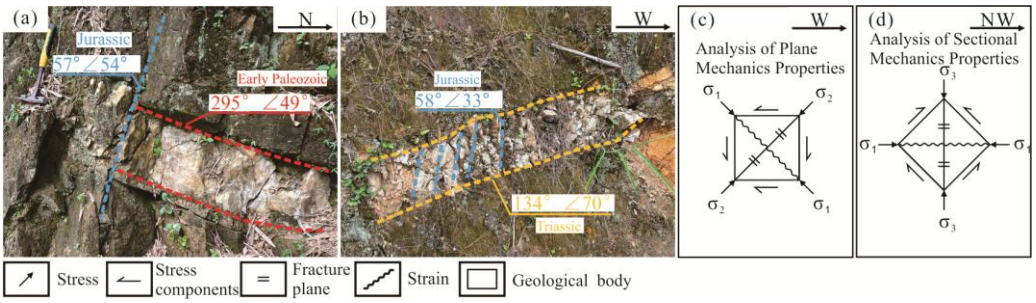


Figure 11. (a) Two different stages of cleavages developed in the Cambrian Niujiaohe Formation strata; (b) Multiple sets of quartz veins in the Cambrian Gaotan Formation are observed filling the tensional spaces between two shear planes, forming along early cleavage and fragmented by later cleavage; (c and d) Analysis of plane and sectional mechanical properties of cleavage developed in the Cambrian Niujiaohe Formation strata.

The Cambrian Gaotan Formation preserves excellent examples of this overprinting relationship, with two different sets of cleavages developed on both sides of the NE-SW trending anticline. The early cleavage formed during the Triassic, while the later cleavage formed in the Jurassic. Multiple sets of quartz veins are observed filling the tensile spaces between the two shear planes, initially aligned with the early cleavage, and subsequently fractured along the direction of the late cleavage (Fig. 11b). This complex vein geometry provides direct evidence for progressive deformation under changing stress conditions.

4.4. Cretaceous NW-SE extension

The NW-SE extensional movement during the Cretaceous Epoch further intensified the NE-SW structural contour in western Guangdong, leading to the development of multiple extensional structures and transforming the NE-dipping structures formed during the Triassic Epoch (see supplementary figure). Field evidence for Cretaceous extensional deformation is primarily documented through normal faults and quartz veins filling extensional spaces. Normal fault planes formed during the Cretaceous movement have dip directions of either NW or SE, consistent with NW-SE extension. On the eastern flank of

the NE-SW trending fold, a fault plane with a dip direction of 94°∠ 53° is observed, cutting across cleavage with an occurrence of 223°∠ 31°, with a sliding distance is about 0.5 meter. (Fig. 12a). Similarly, on the western flank of the NE-SW trending fold, a normal fault with a dip direction of 90°∠ 65° intersect a thrust structure with an occurrence of 46°∠ 17° (Fig. 12b). The above-mentioned findings indicate that the tectonic activity responsible for forming these normal faults occurred after the Triassic compression phase and represented an extensional movement fundamentally different from the preceding Jurassic compression.

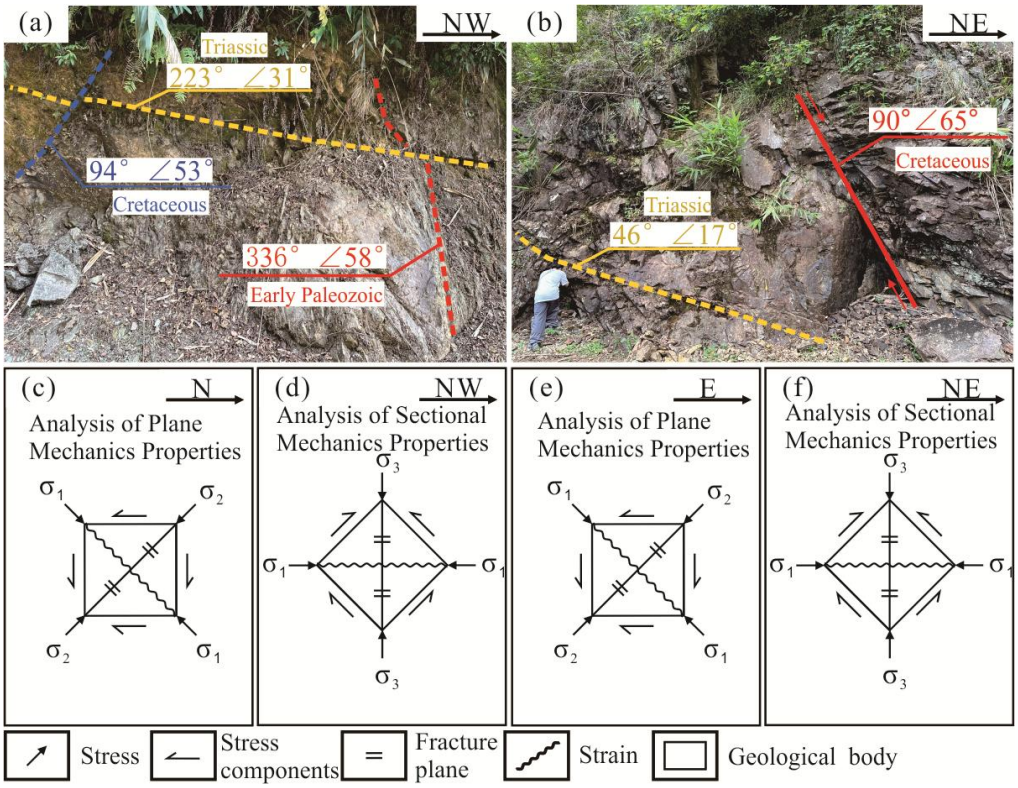


Figure 12. (a) Two different stages of cleavages developed in the Early Paleozoic Gaotan Formation, with the later cleavage intersecting a normal fault characterized by a descending hanging wall and an ascending footwall; (c and d) Analysis of sectional and plane mechanical properties of the fault plane in the Cambrian Gaotan Formation strata; (b) A set of cleavages in the Early Paleozoic Niujiaohe Formation with a steeply dipping fault developing above it; (e and f) Analysis of sectional and plane mechanical properties of the fault plane in the Early Paleozoic Niujiaohe Formation.

Multiple shear quartz veins observed in the Cambrian Niujiaohe Formation strata on the eastern flank of the NE-SW trending fold (Fig. 13), provide additional evidence for extensional deformation. These veins show downward shear in the hanging wall and upward shear in the footwall, with shear planes dipping toward the NW. The quartz veins are slightly inclined relative to the shear plane, suggesting that the extensional movement during this period occurred after the NW-SE compression movement of the Jurassic but shared similar structural characteristics. These observations collectively indicate that western Guangdong experienced significant NW-SE extensional activity during the Cretaceous.

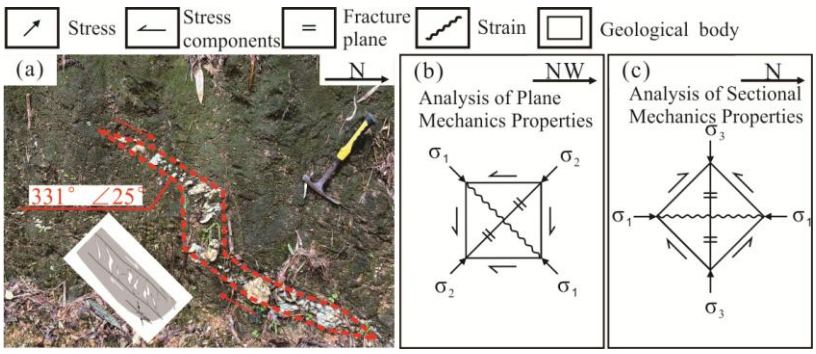


Figure 13. (a) A set of shear quartz veins developed in the Cambrian Niujiaohe Formation, showing descending hanging wall and a rising footwall; (b and c) Analysis of sectional and plane mechanical properties of shear quartz veins in the Niujiaohe Formation strata.

5. The Enlightenment of Structural Evolution Process on Mineralization

So how to use the structural analysis to conduct ore prospecting? Taking the Huangnikeng gold deposit as an example, the ore bodies in this mining area are distributed along both NW-SE and NE-SW trends (Fig. 14), with the majority dipping in the NE-SW direction. Structural analysis reveals that the NE-SW trending ore bodies are controlled by multi-stage structural reactivation, including the Early Paleozoic NW-SE compression, Jurassic NW-SE compression, and Cretaceous NW-SE extension. These complex interactions make the NW-SE trending ore bodies a priority focus for prospecting in the study area. In contrast, the NE-SW structures are mainly controlled by Triassic NE-SW compression and were locally reactivated during the Jurassic-Cretaceous period, showing relatively weak prospecting potential. In addition, the NW-SE trending ore bodies are mainly influenced by Triassic NE-SE compression and were locally reactivated during the Jurassic-Cretaceous period, resulting in comparatively lower prospecting potential. Additionally, the interspersing of NW-SE and NE-SW trending ore bodies suggests that the intersections of these fault structures are highly conductive to ore bodies formation and should be prioritized as key areas for mineral prospecting.

The length of a single ore body ranges from 45 to 800m. The average true thickness of a single ore body varies between 0.81 and 2.6m. The ore bodies are mainly vein-shaped, displaying occasional branching and expansion. Overall, the main ore body shows stable structural characteristics (Fig. 14)[18].

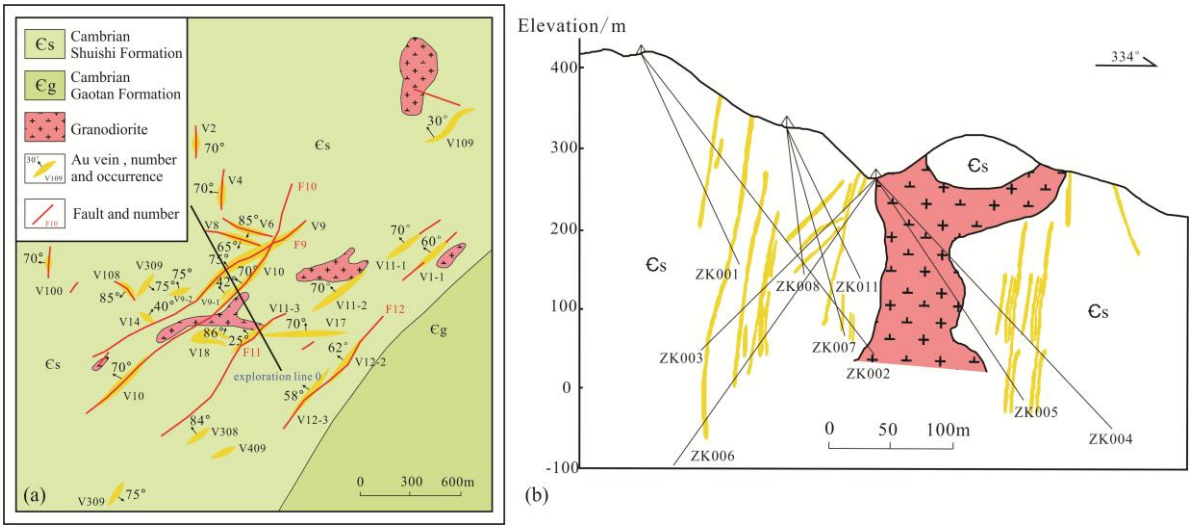


Figure 14. Huangnikeng mining area plan and 0 exploration line profile.

Cross-sectional analysis reveals that ore bodies dipping in the NE-SW direction show signs of higher gold grades compared to the ore bodies. This relationship confirms that the NE-SW trending ore bodies, which are controlled by the combined tectonic movements of the Early Paleozoic NW-SE compression, Jurassic NW-SE compression, and Cretaceous NW-SE extension, possess advanced mineralization potential (e.g., F9 and F11 in figure 14). Therefore, the NE-SW trending structure controlled by the combined tectonic movement of NW-SE trending compression in Early Paleozoic, NW-SE trending compression in Jurassic and NW-SE trending extension in Cretaceous should be the priority prospecting target.

The occurrence, shape and scale of the ore bodies at the Huangnikeng gold deposit are strictly controlled by the fault zone. The NE-trending fault zone is the main ore-conducting and ore-hosting structure of the mining area. The ore-bearing host rock is mainly Cambrian strata, enriched in gold and other ore-forming elements, which provides a material source for the formation of the Huangnikeng gold deposit [19, 20]. In the Cambrian strata, the useful ore-forming elements such as gold were activated by regional metamorphism and magmatic activity, and migrated to the favorable parts of the NE-trending fault zone to form enrichment [21]. The magmatic activity in Jurassic-Cretaceous caused the local expansion of the NE-trending fault zone, and the ore-forming materials carried by it entered, which provided a sufficient heat source for the activation and transfer of ore-forming materials and formed ore-bearing hydrothermal solution [22]. The NE-trending fault zone provides channels and places for the upward migration of ore-bearing hydrothermal fluids and the crystallization and precipitation of metal minerals [18]. In summary, the Huangnikeng gold deposit is a fault-controlled, altered-rock type deposit of hydrothermal origin. The gold in the Huangnikeng gold deposit is mainly filled in the interstitial space of pyrite or arsenopyrite grain aggregates or occurs as native gold in high-grade ore zones [18]. Notably, gold grades increase significantly where pyrite coexists with or is intergrown with late-stage quartz veinlets, indicating continued metal precipitation during late-stage fluid evolution [18]. Previous studies indicate that gold mines with similar mineralization are controlled by tectonic and structural factors, rather than being directly associated with granitoid intrusions [23,24]. The Jurassic-Cretaceous fault structures in the region have undergone a transition from compression to extension, resulting in the development of brittle fault structures. These structures play a crucial role in controlling the migration and precipitation of gold-bearing fluid, creating favorable conditions for gold mineralization [25]. These brittle faults serve as the primary host structures for gold deposits.

The relationship between gold deposits and brittle shear zones is significant, as these shear zones act as both guiding and hosting structures for mineralization [26]. Most gold ore belts or fields in the western Guangdong region are spatially associated with the NE-trending Guangning-Luoding regional deep fault zone, which has experienced ductile shear deformation in deep crustal environments during its early evolution. During the later stages of tectonic evolution, the inherited brittle shear zone systems were superimposed onto the pre-existing ductile shear zones, creating favorable conditions for overprinted mineralization (Fig. 15). According to the prospecting results in the Huangnikeng area, gold deposits are primarily distributed within NW and NE-trending brittle shear zones. High-grade gold deposits are predominantly found at the intersections of these NW and NE-trending brittle shear zones. The Jurassic-Cretaceous tectonic activity marked a transition from compression to extension, leading to significant development of brittle fracture structures that serve as the primary hosts for gold deposits. Based on this, key prospecting targets for gold deposits in this region include: 1. areas controlled by dome structures overlying Jurassic-Cretaceous plutonic intrusions; 2. intersections of NE

and NW trending structural zones. In the light of these findings, specific areas (the target areas) for prospecting have been identified (Fig. 16).

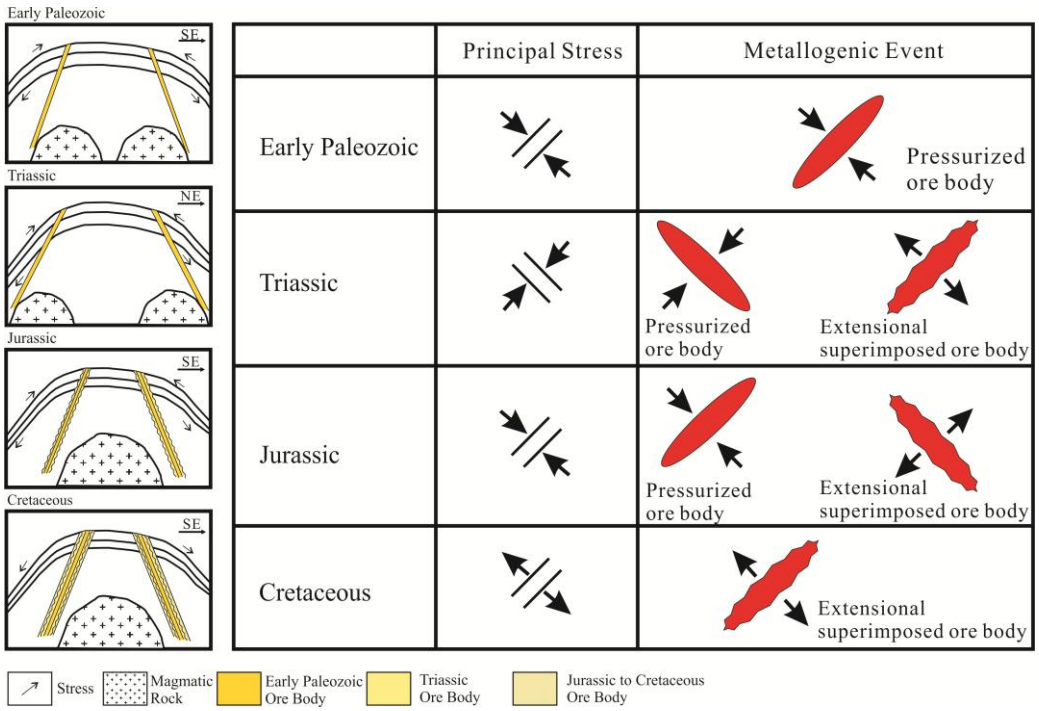


Figure 15. Regional structure ore-controlling model diagram.

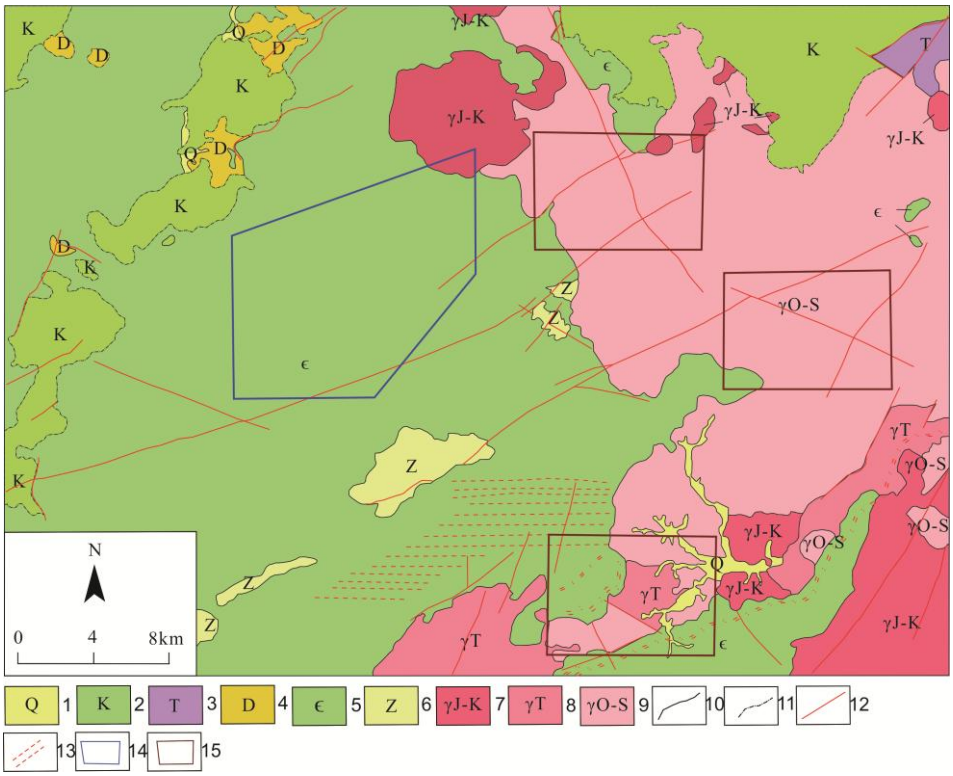


Figure 16. Geological sketch of Huangnikeng-Fengmu area in the western Guangdong region: 1- Quaternary system; 2- Cretaceous system; 3- Triassic system; 4- Devonian system; 5- Cambrian system; 6- Sinian system; 7- Jurassic-Cretaceous granite; 8-Triassic granite; 9- Early Paleozoic granite; 10- Integrate geological boundaries; 11- Inconsistent geological boundary; 12- Fault; 13- (brittle) ductile shear zone; 14- Research area; 15- Target area [27].

6. Conclusions

The western Guangdong region preserves a detailed record of four major tectonic events spanning the phanerozoic: 1. Early Paleozoic NW-SE compression; 2. Triassic NE-SW compression; 3. Jurassic NW-SE compression; 4. Cretaceous NW-SE extension. Each episode is characterized by distinctive structural assemblages and paleo-stress configurations that provide insights into the regional geodynamic evolution and record the progressive evolution of the South China Block. Gold deposits in the region are mainly controlled by multi-stage structural reactivation, with the most favorable targets located at intersections of NW and NE brittle shear zones and fault systems. The transition from compression to extension during the Jurassic-Cretaceous created optimal conditions for extensive brittle structures and hydrothermal fluid circulation. Such processes are fundamental to gold formation. Areas characterized by structural complexity, multiple reactivation events, and proximity to Jurassic-Cretaceous intrusions represent the highest priority exploration targets. More specifically, effective deep mineral prospecting should focus on the influence of dome structures and the intersection of NE and NW-trending structural zones. The future work will focus on geochemical and chronological studies, providing more accurate chronological evidence for the tectonic evolution results obtained by structural analysis, and revealing the source of ore-forming materials and the evolution process of ore-forming fluids.

Author Contributions: Conceptualization, W.Q., T.X. and H. L.; Formal analysis, W.Q.; Funding acquisition, W.Q., T.X. and H. L.; Investigation, W.Q., T. X., Y. H., Z. S., H.L., and B.W.; Methodology, W.Q. and Y. H.; Project administration, W. Q.; Supervision, B.W. and H.L.; Validation, H.L., Y. H. and M.A.E.I.; Writing – original draft, W.Q., H.L., Y.H., B.W. and Z. S.; Writing – review & editing, B.W., H.L., Y. H. and M.A.E.I.. All authors have read and agreed to the published version of the manuscript.

Funding: This research was funded by Changsha General Survey of Natural Resources Centre, China Geological Survey, grant number DD20243181.

Data Availability Statement: Data is provided within the manuscript or supplementary information files.

Acknowledgments: Research funds from China Geological Survey is thanked.

Competing interests: The author(s) declare no competing interests.

References

1. Zhang, S.; Li, T.J.; Wang, L.K. Thermodynamic modelling of ore–forming mechanism of the changkeng gold–silver deposits in guangdong province. *Acta Geologica Sinica - English Edition* 2010, 71(4):433-445.
2. Tian, M.Y; Di, Y.J. Petrogenesis of Jurassic granitic rocks in South China Block: implications for events related to subduction of Paleo-Pacific plate. *Open Geosciences* 2024, 16(1).
3. Zhao, H.J.; Leon, B.; Yuan, S.D.; Zheng, W.; Yu, Z.F.; Guan, B.T. Genesis of the vein-type Gaocheng Ag-Pb-Zn deposit in the western Guangdong province of China and its implication for regional exploration. *Ore Geology Reviews* 2021, 104137-.
4. Wang, B.; Li, H.; Sun, Z.; Quan, W.; Huang, Y.; Faisal, M.; Yingde–Guangning granitic plutons record complex tectonic evolution during Paleozoic-Mesozoic: implications for gold exploration in western Guangdong, South China. *Minerals* 2024, 14(12), 1259.
5. Xiao, Z.C.; Wang, S.; Qi, S.H.; Kuang, J.; Zhang, M.; Li, H.L. Crustal thermo-structure and geothermal implication of the Huangshadong geothermal field in Guangdong province. *Journal of Earth Science* 2023, 34(1), 194-204.
6. Kong, J.T.; Xu, Z.J.; Cheng, R.H.; Wan, D. Provenance of the southeastern South China Block in the Late Triassic and initiation of Paleo-Pacific subduction: evidence from detrital zircon U-Pb geochronology. *JOURNAL OF EARTH SCIENCE* 2024, 35(5), 1426-1446.
7. Peng, S.B.; Zhang, Y.M.; Zhan, M.G.; Chen, F.W.; Qiu, R.Z. Sm-Nd, Pb-Pb and Rb-Sr isotopic dating and its dynamic implications for the proterozoic Augen granite in the Yunkai area, western Guangdong province. *Acta Geologica Sinica - English Edition* 2010, 74(2):289-296.
8. Geng, H.Y.; Xu, X.S.; O'Reilly, Y.S.; Zhao, M.; Sun, T. Cretaceous volcanic-intrusive magmatism in western Guangdong and its geological significance. *Science in China Series D* 2006, 49(7):696-713.
9. Chugaev, V.A. Orogenic gold deposits of northern Transbaikalia, Russia: geology, age, sources, and genesis. *geochemistry international* 2024, 62(9):909-978.

10. Konopelko, D.; Klemd, R.; Petrov, S.V.; Apayarov, F.; Nazaraliev, B.; Scherstén, A.; Sergeev, S. Precambrian gold mineralization at Djamgyr in the Kyrgyz Tien Shan: tectonic and metallogenic implications. *Ore Geology Reviews* 2017, 86537-547.

11. Wang, M.F.; Zhang, X.B.; Pi, D.H.; Guo, X.N. Zircon U–Pb dating of Pubei granite and strontium isotope from sphalerite of the Xinhua Pb–Zn–(Ag) deposit, Yunkai area of Guangxi province, South China. *Acta Geochimica* 2016, 35(2):156-171.

12. Ni, J.L.; Liu, J.L.; Wang, J.C.; Tang, X.L.; Wang, Z.; Li, Z.S.; Li, D.P. Ductile shear deformation and gold mineralization in the Hetai goldfield of the Yunkai massif, South China block. *Geological Journal* 2019, 54(2):929-945.

13. Wang, X.; Liang, H.; Shan, Q. Confirmation and significance of Early Paleozoic metallogenic epoch for gold deposits in South China. *Chinese Journal of Geochemistry* 2001, 20(4):296-301.

14. Yu, Z.F.; Zhang, Z.Q.; Chen, M.H.; Zhao, H.J. Fluid Inclusion characteristics of the Dajinshan W-Sn polymetallic deposit in Yunfu, Guangdong province. *Acta Geologica Sinica - English Edition* 2014, 88(s2):1194-1194.

15. Deng, T.; Xu, D.R.; Chi, G.X.; Wang, Z.L. Chen, G.W.; Zhou, Y.Q.; Li, Z.H.; Ye, T.W.; Yu, D.S. Early Paleozoic (Early Paleozoic) veins overprinted by Yanshanian (Late Mesozoic) gold mineralization in the Jiangnan Orogen: a case study on gold deposits in northeastern Hunan, South China. *Ore Geology Reviews* 2020, 124.

16. Hong, J.X.; Zhai, D.G.; Keith, M. Quartz texture and the chemical composition fingerprint of ore-forming fluid evolution at the Bilihe porphyry Au deposit, NE China. *American Mineralogist* 2024, 109(7):1203-1219.

17. Wang, B.; Li, H.; Sun, Z.; Quan, W.; Huang, Y. Yingde– Guangning granitic plutons record complex tectonic evolution during Paleozoic-Mesozoic: implications for gold exploration in western Guangdong, South China. *Minerals* 2024, 14(12):1259-1259.

18. Wang, L.; Xu, D.; Zhang K.; Hu Jun.; Xiao G.; Xu J. Geological and geochemical characteristics and metallogenic epoch of Huangnikeng gold deposit in western Guangdong. *Mineral deposits* 2017, 02-0317-13.

19. Taylor, S .R.; McLennan, S.M. The continental crust: Its composition and evolution. *Oxford: Blackwell Scientific Publications* 1985, 57-72.

20. Taylor, S. R.; McLennan, S.M. The geochemical evolution of the continental crust. *Reviews of Geophysics* 1995, 33(2): 241-265.

21. He, J. Preliminary study on metallogenic geological background of gold deposits in western Guangdong. *Nonferrous Metals Engineering* 2003, 55(3):25-28.

22. Xu, Y.; Luo, Y.; Xiao, G.; Luo, D.; Hu, Y. Brief analysis of geological characteristics and genesis of the Huangnikeng gold deposit in western Guangdong. *South China Geology* 2012, 28(4):369-375.

23. Jiang, S.Y.; Ma, Y.; Liu, D.L.; Li, W.T. Orogenic gold deposits: mineralization mechanism and research perspectives. *Journal of Earth Science* 2023, 34(06):1758-1761.

24. Heo, C.H.; Yun, S.T.; So, C.S.; Choi, S.G. Geochemistry of the granitoids hosting the Seolhwa Au mine, Asan district, Chungcheongnamdo province, Korea: Genetic implication on the mesothermal gold mineralization. *Geosystem Engineering* 2002, 5(2):54-66.

25. Shawky, N.B. Intrusion-related gold deposits in Egypt. *Acta Geologica Sinica - English Edition* 2021, 95(3):1033-1055.

26. Ganguly, S.; Manikyamba, C.; Saha, A.; Lingadevaru, M.; Santosh, M.; Rambabu, S.; Khelen, A.C.; Purushotham, D.; Linga, D. Geochemical characteristics of gold bearing boninites and banded iron formations from Shimoga greenstone belt, India: implications for gold genesis and hydrothermal processes in diverse tectonic settings. *Ore Geology Reviews* 2016, 7359-82.

27. Lu, S.H.; Li, J.G.; Li, J. The geological characteristics and prospecting prediction of gold deposits in the Huangnikeng-Fengmu area, western Guangdong province. *Mineral Exploration* 2023, 14(12):2316-2327.

Disclaimer/Publisher's Note: The statements, opinions and data contained in all publications are solely those of the individual author(s) and contributor(s) and not of MDPI and/or the editor(s). MDPI and/or the editor(s) disclaim responsibility for any injury to people or property resulting from any ideas, methods, instructions or products referred to in the content.

Supplementary Files

This is a list of supplementary files associated with this preprint. Click to download.

- supplementaryfigure.pdf